



Article

Structural and Functional Annotation of Transposable Elements Revealed a Potential Regulation of Genes Involved in Rubber Biosynthesis by TE-Derived siRNA Interference in *Hevea brasiliensis*

Shuangyang Wu^{1,2,3,4} , Romain Guyot^{5,6} , Stéphanie Bocs^{1,2,7} , Gaëtan Droc^{1,2,7} , Fetrina Oktavia⁸, Songnian Hu^{4,9}, Chaorong Tang¹⁰, Pascal Montoro^{1,2} and Julie Leclercq^{1,2,*}

- ¹ CIRAD, UMR AGAP, F-34398 Montpellier, France; shuangyangwu@foxmail.com (S.W.); stephanie.sidibe-bocs@cirad.fr (S.B.); gaetan.droc@cirad.fr (G.D.); pascal.montoro@cirad.fr (P.M.)
- ² AGAP, University Montpellier, CIRAD, INRA, Institute Agro, F-34398 Montpellier, France
- ³ State Key Laboratory of Integrated Management of Pest Insects and Rodents, Institute of Zoology, Chinese Academy of Sciences, Beijing 100101, China
- ⁴ University of Chinese Academy of Sciences, Beijing 100049, China; husn@im.ac.cn
- ⁵ Institut de Recherche pour le Développement, University Montpellier, UMR DIADE, 34394 Montpellier, France; romain.guyot@ird.fr
- ⁶ Department of Electronics and Automatization, Universidad Autónoma de Manizales, 170001 Manizales, Colombia
- ⁷ South Green Bioinformatics Platform, Bioversity, CIRAD, INRA, IRD, F-34398 Montpellier, France
- ⁸ Indonesian Rubber Research Institute, Sembawa Research Centre, 30953 Palembang, Indonesia; fetrina_oktavia@yahoo.com
- ⁹ State Key Laboratory of Microbial Resources, Institute of Microbiology, Chinese Academy of Sciences, Beijing 100101, China
- ¹⁰ College of Tropical Crops, Hainan University, Haikou 570228, China; chaorongtang@hainanu.edu.cn
- * Correspondence: julie.leclercq@cirad.fr

Received: 5 May 2020; Accepted: 11 June 2020; Published: 13 June 2020



Abstract: The natural rubber biosynthetic pathway is well described in *Hevea*, although the final stages of rubber elongation are still poorly understood. Small Rubber Particle Proteins and Rubber Elongation Factors (SRPPs and REFs) are proteins with major function in rubber particle formation and stabilization. Their corresponding genes are clustered on a scaffold1222 of the reference genomic sequence of the *Hevea brasiliensis* genome. Apart from gene expression by transcriptomic analyses, to date, no deep analyses have been carried out for the genomic environment of SRPPs and REFs loci. By integrative analyses on transposable element annotation, small RNAs production and gene expression, we analysed their role in the control of the transcription of rubber biosynthetic genes. The first in-depth annotation of TEs (Transposable Elements) and their capacity to produce TE-derived siRNAs (small interfering RNAs) is presented, only possible in the *Hevea brasiliensis* clone PB 260 for which all data are available. We observed that 11% of genes are located near TEs and their presence may interfere in their transcription at both genetic and epigenetic level. We hypothesized that the genomic environment of rubber biosynthesis genes has been shaped by TE and TE-derived siRNAs with possible transcriptional interference on their gene expression. We discussed possible functionalization of TEs as enhancers and as donors of alternative transcription start sites in promoter sequences, possibly through the modelling of genetic and epigenetic landscapes.

Keywords: transposable elements; siRNA; rubber tree; transcriptional regulation; epigenomics

1. Introduction

Natural rubber biosynthetic pathway was very recently reviewed by [1]. *Hevea brasiliensis* is a sole tropical perennial crop used for the industrial production of natural rubber (NR) [2]. Selected clones, for latex and/or timber production, are propagated by grafting. The cis-1,4 polyisoprene is biosynthesized from sucrose produced by photosynthesis in the leaves and translocated to specialized cells called laticifers. After loading, sucrose is metabolized into isopentenyl pyrophosphate (IPP), a monomer used for elongation of the polymer biosynthesized in the rubber particles of latex cells [3]. All genes involved in the NR biosynthesis pathway have been identified in the genomic sequences of the Chinese rubber clone Reyan 7-33-97 [4], and particularly the genes encoding the Rubber Elongation Factor (*REF1–8*) and Small Rubber Particle Protein (*SRPP1–10*) families. *SRPPs* were identified in many plants (rubber and non-rubber producing), while *REFs* were not found in other plants [1]. They have been shown to be more extended in *Hevea* compared to other rubber-producing plants [4,5], probably due to a whole genome duplication shared with cassava (*Manihot esculenta*), another *Euphorbiaceae* plant species [6]. Among various clones, *REF* transcript levels have been shown to be positively correlated with latex yield [7]. In addition, clonal phenotypic properties exit as they are classified according to the biochemical ability of latex cells to produce rubber assessed by their sucrose, thiols and inorganic phosphorus contents. Sucrose content reflects the balance between sucrose consumption by the latex cells for energy production, latex biosynthesis, and the transfer of sucrose from the apoplast to the latex cells. Inorganic phosphorus content indicates the intensity of metabolic activity in the latex cells [8,9]. The thiol content reflects the redox status of the tree, namely the level of control of the oxidative stress of trees under production [10–13]. These three parameters are actually used for a good management of the plantation such as tapping frequency and ethephon stimulation [14]. In case of overexploitation of *Hevea* by excessive tapping or stimulation with ethephon, physiological disorders appear leading to Tapping Panel Dryness (TPD). This clone-dependent physiological disease [15,16] is characterized by oxidative stress in laticifers, leading to a cessation of latex flow with in situ coagulation of rubber (for review [13,17]).

In addition to biochemical data, we have access to a transcriptomic data. For example, the transcripts *REF1*, *REF3*, *REF7* and *SRPP1* are strongly expressed in the laticifers in the clone Reyan 7-33-97. In contrast, transcripts from other families of *SRPPs* (*SRPP3*, *SRPP5*, *SRPP8* and *SRPP9*) and *REFs* (*REF2*, *REF4*, *REF5*, *REF6* and *REF8*) were detected at low levels in latex. By contrast, in clone RRIM 600, *REF2*, *REF3*, *REF7*, *REF8* and *SRPP1* are the most highly expressed in latex [18]. Beyond a differential contribution of *REF* and *SRPP* isoforms to NR biosynthesis between clones, possible transcriptional control has been suggested, as in clone RRIM 600 some of the natural rubber biosynthetic genes displayed an alternative transcription start site (TSS), in a tissue-dependent manner [18].

Several *de novo* genomes of rubber clones, with contrasting latex physiology, are available such as Reyan 7-33-97 [4], RRIM 600 [18], BPM 24 [19]; PB 260 [20,21] and GT 1 [5]. The rubber tree genome is large and complex to assemble because of its high heterozygosity, whole genome duplication and transposable element (TE) content [4,5]. TEs, first described in 1931 by the Nobel Prize winner Barbara McClintock, are also known as “jumping genes”. Transposition is often neutral, but their mutagenic potential is now demonstrated through genetic and epigenetic mechanisms, in the establishment and/or alteration of gene regulatory networks, in the modification of phenotypes and in the possible generation of adaptive genetic variations [22]. TE exaptation, which is the transformation of the repeated elements into a novel host gene, or a promoter region, is consistent with their role as “engines of plant genome evolution” [23,24]. TEs are classified hierarchically by subdividing them into Classes, Orders, Super-families, Lineages and Families [25]. Class I, corresponds to retrotransposons (LTR (Long Terminal Repeat), PLE, LINE (Long Interspersed Nuclear Element) and SINE (Short Interspersed Nuclear Element)), while Class II comprises DNA transposons (TIR (Terminal Inverted Repeat), Crypton, Helitron and Maverik). This classification system has been successfully used in the TE classification of several plant species [25–31]. In plant genomes, LTR retrotransposons are present in large numbers and classified according to the protein sequence [32], with two evolutionary distinct Superfamilies, *Ty3/gypsy* (*Athila*, *Tat*, *Galadriel*, *Reina*, *CRM/CR*, and *Del/Tekay* among others)

and *Ty1/copia* (*TAR/Tork*, *Angela/Tork*, *Ikeros/Tork*, *Maximus/Sire*, *Ivana/Oryco*, *Ale/Retrofit* and *Bianca*, among others) [33]. However, the transcription and movement of these retroelements have been observed in response to development and environmental cues, due to the presence of *cis*-regulatory patterns, which could facilitate plant adaptation by giving new regulatory patterns to genes [23]. Small interfering RNAs (siRNAs), which trigger RNA-directed DNA methylation (RdDM), effectively silence TEs [34]. Our previous studies on populations of small RNAs in *Hevea* clone PB 260 showed alterations in the microtranscriptome of laticifers in response to environmental cues and TPD [35]. A shift in the distribution of small RNAs has been observed, with peaks of small RNAs of 24- and 21-nt, in healthy and TPD-affected trees of clone PB 260, respectively. This suggests a shift from transcriptional regulation in healthy trees to post-transcriptional regulation in trees affected by TPD [35–37]. Very recently, it has been shown that 21-nt small RNAs do not originate from *MIR* genes and could therefore be classified as siRNAs [20]. In addition, given the size of these siRNAs (21-nt), they could be responsible for the degradation of target transcripts by post-transcriptional cleavage, or the maintenance of TE silencing by epigenetically activated small interfering RNAs (easiRNAs) [34].

In this study, we chose PB 260 clone for which genomic [20,21], transcriptomic [17,38,39] and microtranscriptomic data [20,35,37] were available (Figure 1) [4,5,17,18,20,21,35,37–39]. In addition, functional validation could be possible for this clone as the genetic transformation procedure is robustly mastered [40–45]. Our objective was to annotate, in clone PB 260, TEs and siRNAs sharing sequence identity with TEs (namely TE-derived siRNAs as a track of annotation), to infer their possible interference with gene expression in laticifers, and to show TE-transcriptional regulation of genes involved in rubber biosynthesis. Firstly, we carried out in silico detection and accurate annotation on a genome scale of TEs with the REPET and LTR_STRUC pipelines [46] (Figure 2), as only a few active elements have been described in the genus *Hevea* so far [47]. Thus, from the *Hevea* TE database generated, their diversity and activity were further analysed (Figure 1). Secondly, as the majority of the *REF/SRPP* genes were clustered on a single scaffold 1222 [4], this genomic region was curated manually. The capacity of TEs to produce siRNAs was evaluated. Lastly, all this computational information was combined to put forward hypotheses on how genomic/epigenomic environments affect the transcriptional regulation of *REF/SRPP* gene cluster by comparing side-by-side genomic sequences from other clones (PB 260, Reyan 7-33-97, RRIM 600 and GT 1).

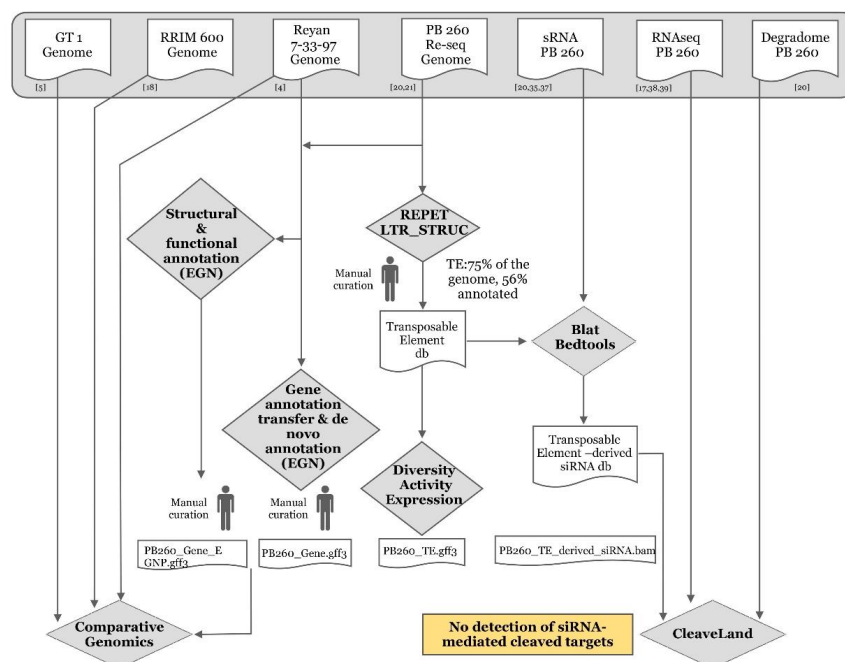


Figure 1. Diagram of the bioinformatics analyses described in this study, and data origins. Numbers refer to references mentioned in the text [4,5,17,18,20,21,35,37–39].

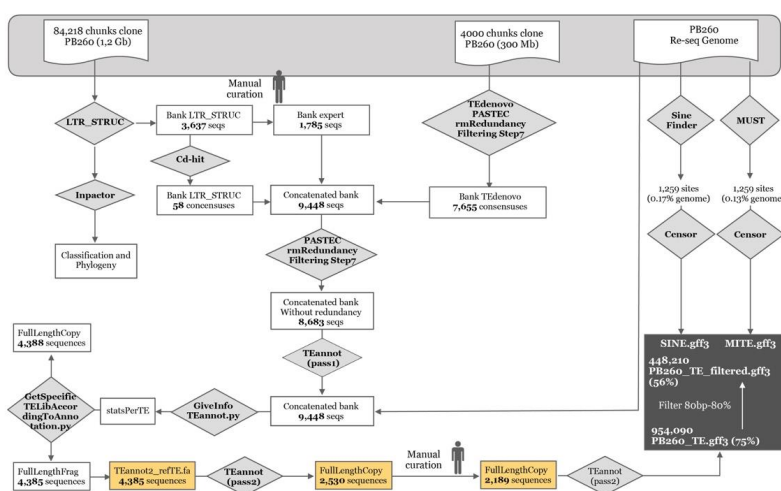


Figure 2. Detailed diagram of the transposable element annotation process implemented by the LTR_STRUCT, REPET pipeline, MUST and Sine_finder.

2. Results

2.1. Transposable Element Annotation Process

To accurately annotate TEs in the re-sequenced genome of rubber clone PB 260, the LTR_STRUCT and REPET pipelines were used (Figure 2). LTR_STRUCT detected 3637 sequences from the 84,128 blocks in the re-sequencing data. Fifty-eight LTR consensus sequences were built and the singletons (1785) were stored in the expert bank. At the same time, 300 Mb of genomic sequences were analysed by the REPET software, which includes the TEdenovo and TEannot pipelines (Figure 2).

TEdenovo detected 7655 consensus sequences, which were added to the expert bank already containing the consensus sequences obtained by LTR_STRUCT (9448 sequences in total). Three TEannot rounds were required. The first two rounds were used to construct libraries of full-length fragments of transposable elements (4385 sequences) and full-length copies of transposable elements (4388 sequences), finally resulting in the detection of 2189 consensus sequences after the second round and the manual curation steps. The third round of analyses was performed to annotate the entire genome, leading to the detection of 954,090 TEs, representing 75% of the genome. After filtering TEs at least 80 bp long and sharing a homology of at least 80% [25], 448,210 TEs were fully annotated, representing 56% of the genome (Figure 2 and Table 1).

Table 1. Statistics of TE annotation of genomic sequences from clone PB 260 by REPET according to Wicker’s classification [25].

PB 260 V1 Assembly	Before Filtering		After Filtering (>79 bp & >79% id)	
	Number	%	Number	%
HX-incomp	1459	0.15	279	0.06
DTX-comp	699	0.07	150	0.03
DTX-incomp	51,214	5.37	20,033	4.47
RIX-comp	2251	0.24	1476	0.33
RIX-incomp	13,529	1.42	10,418	2.32
RLX-comp	86,648	9.08	55,737	12.44
RLX-incomp	587,149	61.54	292,899	65.35
RXX	1902	0.20	1277	0.28
RXX-LARD	122,504	12.84	31,394	7.00
RXX-TRIM	7877	0.83	4162	0.93
Total TE length (bp)	875,232		417,825	
Total TE (% genome)	74.49		56.55	

2.2. Composition of the Genome in TEs, Their Diversity and Activity

Complete and incomplete TEs were classified according to their Orders and Superfamilies, as described in [25]. In rubber, the largest Order consists of the LTR retrotransposons (RLX in Table 1). LTRs represent more than 77% of TE length in the genome sequence of clone PB 260. Far behind, the Large Retro-transposon Derivatives (RXX-LARD) Order/Superfamily represented 7%. MITE (Miniature Inverted-repeat Transposable Element, 0.13% of TE) and SINE (0.17% of TE), with less than 1700 copies each, were annotated separately with more specific pipelines, namely MUST and Sine_finder (Figure 2). Since most TEs belonged to the LTR Order, a complete phylogenetic analysis, based on amino acid sequences from the reverse transcriptase (RT) domain, when present, was carried out on 1476 full-length copies obtained after LTR_STRUC and Inpactor classification with nine major lineages of LTR retrotransposons, of which 4 and 5 belonged to the *Ty1/copia* and *Ty3/gypsy* superfamilies, respectively (Supplementary Figure S1). In addition, the representativeness of the diversity of LTRs was not affected by the manual curation step of the consensus sequences predicted with REPET, as shown by the complete phylogenetic analysis carried out before and after manual curation (Supplementary Figure S2A,B). Lastly, at genome-wide level, a significant fraction of the *Hevea* genome was composed of LTR *Ty3/gypsy* elements and more particularly the *Del/Tekay* groups, with more than 9129 elements (9129/11,989; 76.1% of RT domains) (Figure 3).

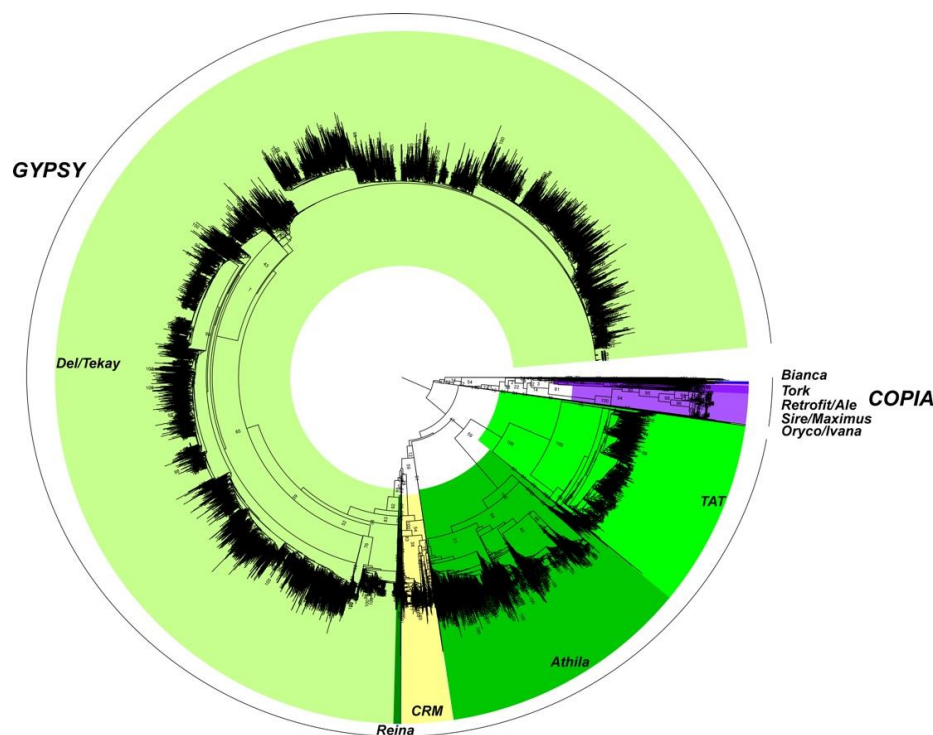


Figure 3. Quantitative representation, on a genome scale, of LTR retrotransposon RT domains in the *H. brasiliensis* PB 260 genomic sequences. The phylogenetic analysis was carried out with reverse transcriptase (RT) domains (19,151) having a length > 200 aa and amino-acid identity > 70% compared to the RT reference domains downloaded from GyDB. The *Gypsy* LTR retrotransposon clades are represented in different green and yellow colours. The *Copia* LTR retrotransposon clades are represented in purple.

LTR transposition is based on the production of polyadenylated RNA molecules through the presence of a site for *RNA pol II* inserted in the 5' UTR region and a polyadenylation site in the 3' UTR region [48]. The timing of insertion of full-length LTR retrotransposons was measured by calculating the divergence of LTRs of the same elements and estimating the time using a substitution rate for *Hevea*. The most recently inserted elements shared a high level of similarity between their LTRs.

Older inserted elements showed more mutations in their sequences. Each *superfamily* and lineage of full-length retroelements was characterized and their insertion times estimated (Figure 4). As shown in Figure 4A, the *Ty3/gypsy* and *Ty1/copia* superfamilies had different insertion times, *Ty1/copia* showing more recent insertions than *Ty3/gypsy*. At lineage level, no *Ty3/gypsy* lines had recently been inserted despite the massive presence of LTRs from the *Del/Tekay* line (Figure 4B), while the *Retrofit/Ale* lines were the most recently added *Ty1/copia* elements (Figure 4C). In the available RNA-seq data from latex [39], none was found to be differentially expressed in response to ethephon or ethephon-induced TPD (Supplementary data 1).

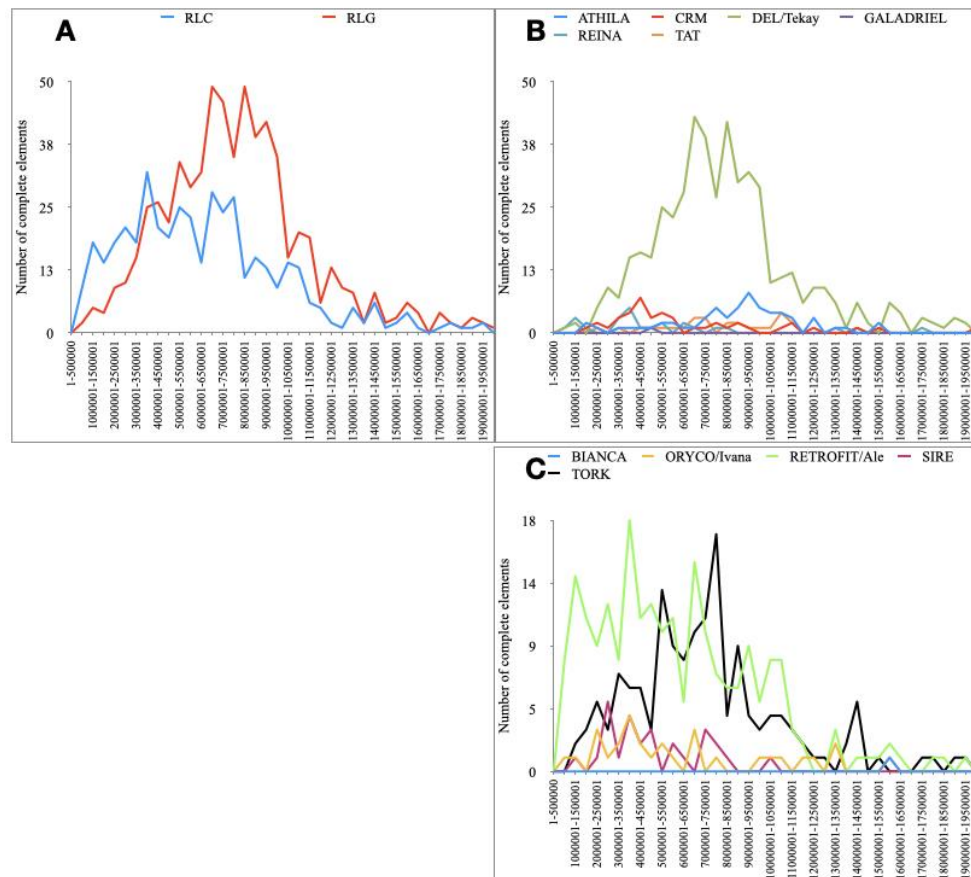


Figure 4. Timing of full-length LTR retrotransposon insertions into the *H. brasiliensis* clone PB 260 genomic sequence. (A) Blue and red lines represent, respectively, the number of *Ty1/copia* (RLC) and *Ty3/gypsy* (RLG) full-length LTR retrotransposons per bins of 0.5 Million Years (MY). (B) Coloured lines represent the number of full-length *Ty3/gypsy* (RLG) LTR retrotransposon lineages per bins of 0.5 MY. (C) Coloured lines represent the number of full-length *Ty1/copia* (RLC) LTR retrotransposon lineages per bins of 0.5 MY. Only the full-length LTR retrotransposons found by LTR_STRUC were used here. An average substitution rate of 3.89×10^{-9} was used.

2.3. Annotation of TE-Derived siRNAs

Small RNAs aligning with TE sequences were further annotated as TE-derived siRNAs then classified according to their size (Figure 5, Supplementary data 2). The majority of siRNAs derived from TEs had a size of 23 and 24 nt (above 35% of total reads), followed by size classes of 22 (15%) and 21 nt (10%). Conversely to previous assumptions, no differences in the distribution of siRNAs derived from TEs were observed between young seedlings, healthy trees and trees affected by TPD (Figure 5).

The production of 24-nt siRNA by TE superfamilies was then quantified by counting those that mapped on TE sequences (Figure 6, Supplementary data 2). The LTR retrotransposon order produced the largest number of siRNAs (70%), with 33% of them by *Ty3/gypsy* -RLG, followed by unclassified

retrotransposon RIX (18%) and *Ty1/copia* RLC (16%). The DTX of DNA transposons contributed to about 3% of siRNA production. We further analysed the 24-nt siRNAs production by TEs in three small RNA-seq libraries including young plants, latex from healthy trees and latex from TPD-affected trees [35,37]. Interestingly, there was no significant in siRNAs production by transposable elements between young trees, latex from healthy and TPD-affected trees. The same proportions were observed for 21, 22 and 23 nt (Supplementary Figure S3).

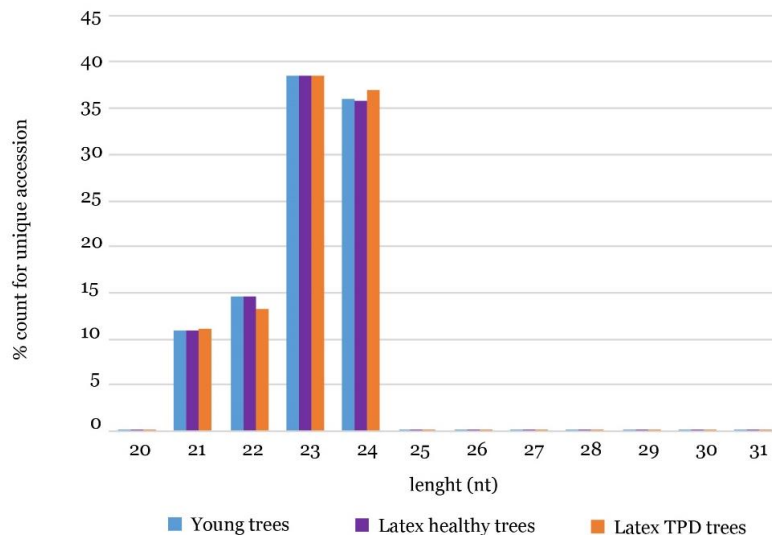


Figure 5. Length distribution of unique TE-derived small RNA accessions from *Hevea* tissues: (young trees (●), latex from healthy trees (●) and latex from TPD-affected trees (●)).

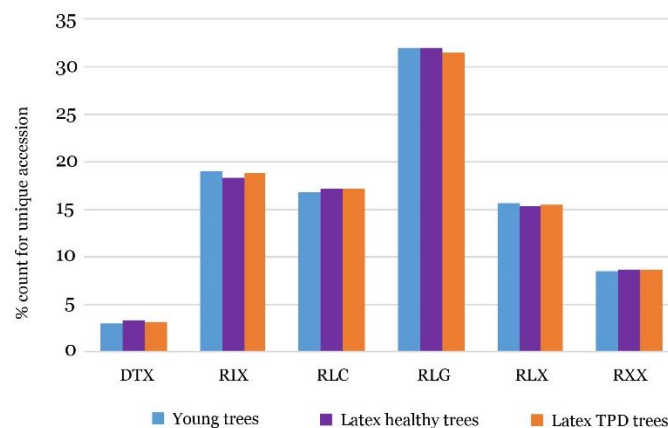


Figure 6. 24-nt siRNA production by transposable element order and superfamilies (%).

To look into possible implication of in post-transcriptional regulation, degradome data were analysed with TE-derived siRNA data sets (20–22 nt), excluding previously identified miRNAs [20]. None of the TE-derived siRNAs with a size of 20–22 nt demonstrated post-transcriptional activity as well as for 24-nt TE-derived siRNA as expected (data not shown).

2.4. Structural and Functional Annotation of a Re-Sequenced Genome from Clone PB 260

To transfer the structural and functional annotation from the Reyan 7-33-97 reference genome to clone PB 260, the EGN-EP transfer pipeline was used [49]. The transfer was successful for 40,241 of the 46,710 Reyan 7-33-97 genes, concerning 3452 scaffolds. The BUSCO evaluation of the completeness of genome annotation showed that EGN transfer was not effective enough to annotate the re-sequenced PB 260 genome with only 81.6% of the complete genes (Supplementary data 3).

their promoters were retained in both clones. Concerning gene expression, in RRIM 600, the highest *REF* transcript expressed was *REF3* and not *REF1* [18]. In the *REF3* genomic region, there was no conservation between RRIM 600 and PB 260 (Figure 8), which could explain the difference in expression level. Conversely, comparative analysis between scaffold 1222 from PB 260 and chromosome 9 from the GT 1 genome indicated a deep restructuring of the *REF/SRPP* locus in GT 1 (Figure 8). In GT 1, the *REF/SRPP* genes were distributed in two loci on chromosome 9 separated by 12 Mb (13.2–13.5 Mb and 1.5–1.6 Mb), which indicate the large difference in *REF/SRPP* genes between these two cultivars. These results may reflect the difference in the ability of two cultivars in rubber biosynthesis.

It is interesting to note that the *SRPP1* gene, strongly expressed in latex with more than 120,000 counts (Table 2), contained a LTR/*Ty1/copia/Retrofit/Ale* (TE6832), almost complete, for which the 3' part of the polyprotein and the 3' LTR were missing in its promoter, without siRNA production. TE6832 was not differentially expressed in response to ethephon-induced TPD (Supplementary data 1). On the other hand, when a large amount of siRNA was detected upstream or downstream of a gene body, the level of expression was considerably reduced, such as *SRPP9*, *SRPP9b* and *SRPP3*, with fewer than 110 counts in each of the biological repeats (Table 2).

Table 2. Normalized read counts for *REF* and *SRPP* transcripts present on scaffold 1222 from latex of clone PB 260 calculated from RNA-seq data for three independent biological replications on healthy trees [39].

Gene Name	Position (bp)	R1	R2	R3
<i>SRPP9</i>	19,366–20,632	51.99	31.99	49.00
<i>SRPP9b</i>	36,463–37,765	14.01	13.01	5.00
<i>SRPP8</i>	54,103–56,474	108.00	126.02	168.00
<i>SRPP1</i>	59,800–61,252	26,2376.06	224,480.10	120,968.96
<i>REF7</i>	88,564–89,747	68,916.89	51,496.25	52,838.13
<i>SRPP3</i>	94,224–95,735	16.95	17.12	106.20
<i>REF3</i>	99,200–100,584	63,213.40	65,499.08	49,443.43
<i>REF2</i>	120,898–122,073	356.01	435.57	509.70
<i>REF4</i>	123,285–124,611	10,012.49	8702.42	15,524.53
<i>REF1</i>	135,970–137,141	509,705.38	452,203.00	392,969.38
<i>REF8b</i>	168,119–168,886	1967.65	1328.53	2174.31
<i>REF8</i>	174,369–175,626	6423.97	5897.50	4242.77
<i>REF5</i>	180,674–181,548	713.99	786.00	568.00
<i>SRPP5</i>	195,438–196,845	689.00	978.98	308.00
<i>partial</i>	203,928–204,179	0.00	0.00	0.00

For the *REF8b* gene, incomplete insertion of LTR was observed in the gene body, leading to the loss of the third exon. This gene is probably no longer functional, even if reads had been detected in the RNA-seq data (Figure 8, Table 2). *REF8b* had a much lower expression level than *REF8*, with fewer than 2500 and more than 4000 counts, respectively (Table 2). On the other hand, analyses of the RNA-seq data showed that the partial sequence, non-annotated and detected at the 3' extremity of the scaffold, was not expressed at all (no count, Table 2).

Cis-regulatory elements in the promoter sequences were detected in highly, moderately and weakly expressed gene (Table 3). The strong expression of the *SRPP1* gene associated with the presence of a large number of enhancer pattern (14) brought by the transposon located in the promoter region. The *REF1* and *REF8* genes have an identical number of enhancer motifs (4) and an expression level varying by a factor of approximately 80, which is not explained by the presence of other motifs. We noted the presence of siRNAs mapping on the exons of the *REF1* gene, and to a much lesser extent for the exons of the *REF8* gene. It is worth mentioning that *cis*-regulatory elements of expression induction under anaerobic conditions were detected in all the promoters tested. However, a diversity of hormone response boxes was observed with members responding to auxin (*REF3–8* and *SRPP5*), ABA (*REF2–5* and *SRPP1*), MeJA (*REF8*) and salicylic acid (*REF3* and *REF4*) (Table 3).

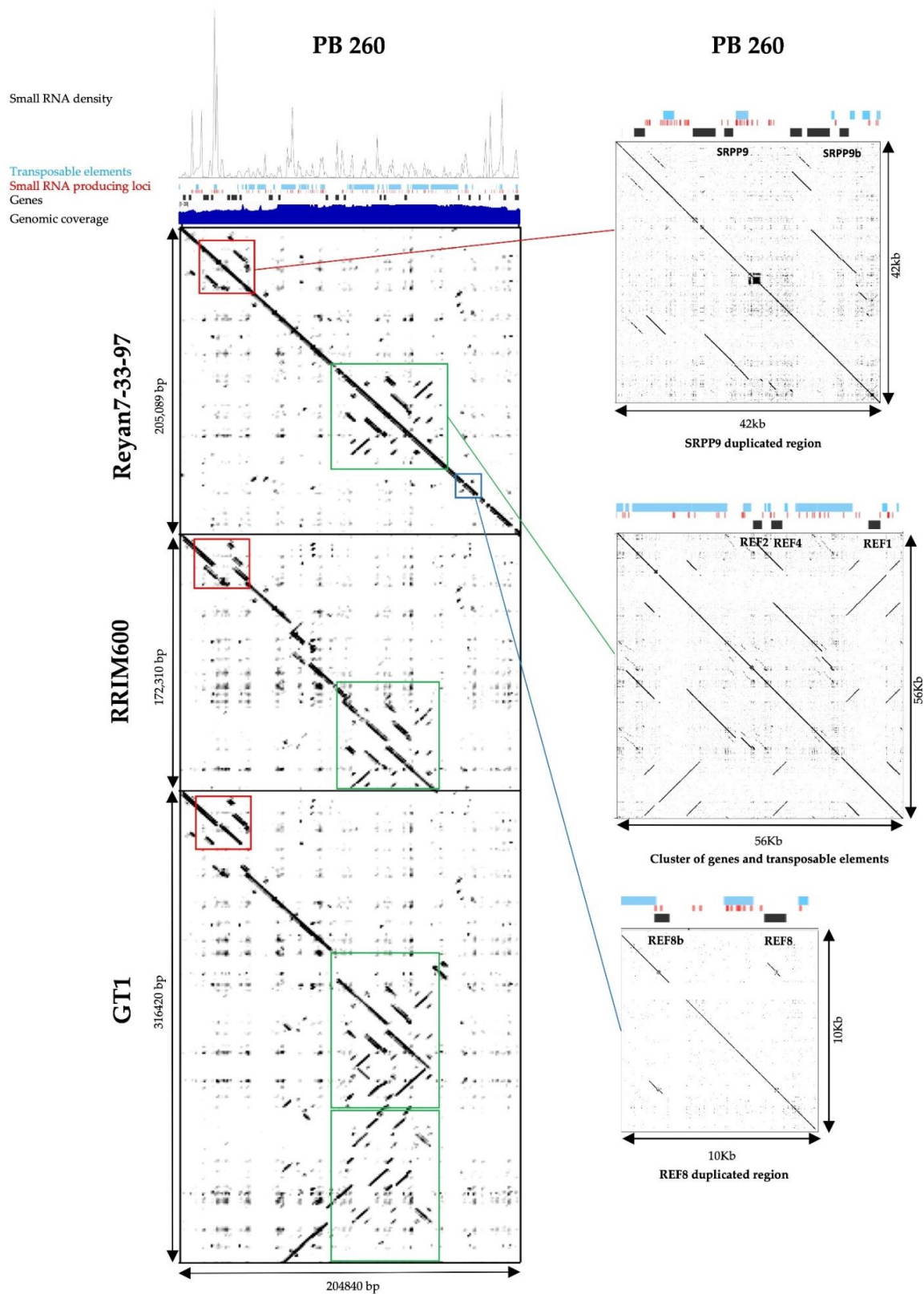


Figure 8. Scaffold 1222 sequence comparison between clones PB 260, Reyan 7-33-97, RRIM 600 and GT 1 by Dot-Plot and genomic DNA read abundance, gene, transposable elements and small RNA density (for PB 260 only). Genomic DNA reads are represented in dark blue, genes in black, transposable elements in light blue, and small RNA in red associated with their density profile. Regions of interest were zoomed in and displayed at the right.

Table 3. Promoter sequence analysis of PB 260 scaffold1222 with the PlantCare tool (<http://bioinformatics.psb.ugent.be/webtools/plantcare/html/>). All the *cis*-regulatory elements found are listed and recorded.

Response to	Motif	Element's Name	REF1	REF2	REF3	REF4	REF5	REF7	REF8	SRPP1	SRPP5
Enhancer	CAAT-box	common <i>cis</i> -acting element in promoter and enhancer regions	4	3	2	2	3	2	4	14	2
light	G-Box	<i>cis</i> -acting regulatory element involved in light responsiveness	1	4	2	2	2	0	0	3	0
	ACE	<i>cis</i> -acting element involved in light responsiveness	1	0	0	0	1	1	1	0	0
	Box 4	part of a conserved DNA module involved in light responsiveness	1	1	8	9	2	0	2	0	1
	MRE	MYB binding site involved in light responsiveness	0	0	1	0	0	0	1	0	0
	GT1-motif	light responsive element	1	0	2	0	0	0	3	0	2
	TCT-motif	part of a light responsive element	0	0	1	1	1	0	0	0	0
	TCA-element	<i>cis</i> -acting regulatory element involved in light responsiveness	0	0	1	1	0	0	0	0	0
	AT1-motif	part of a light responsive module	0	0	0	0	1	0	0	0	0
Anaerobic	ARE	<i>cis</i> -acting regulatory element essential for the anaerobic induction	2	1	2	2	3	1	3	4	1
Hormone	ABRE	<i>cis</i> -acting element involved in abscisic acid responsiveness	0	1	3	1	1	0	0	1	0
	AuxRR-core	<i>cis</i> -acting regulatory element involved in auxin responsiveness	0	0	1	1	0	0	0	0	0
	TGA-element	auxin-responsive element	0	0	1	1	1	1	1	0	1
	AE-box	<i>cis</i> -acting element involved in salicylic acid responsiveness	0	0	1	1	0	0	0	0	0
	CGTCA-motif	<i>cis</i> -acting regulatory element involved in MeJA responsiveness	0	0	0	0	0	0	0	1	0
Abiotic stress	LTR	<i>cis</i> -acting element involved in low-temperature responsiveness	0	0	0	0	0	0	0	2	0
	TC-rich repeats	<i>cis</i> -acting element involved in defence and stress responsiveness	0	0	0	0	0	0	0	1	0
	MBS	MYB binding site involved in drought inducibility	0	0	0	0	0	0	0	1	0
Development	GCN4_motif	<i>cis</i> -regulatory element involved in endosperm expression	0	0	0	0	0	0	0	1	0
	circadian	<i>cis</i> -acting regulatory element involved in circadian control	0	0	0	0	0	0	0	1	0
Others	A-box	<i>cis</i> -acting regulatory element	0	0	0	0	0	0	0	1	0
	O2-site	<i>cis</i> -acting regulatory element involved in zein metabolism regulation	0	0	0	0	0	0	1	0	0
Total			10	10	25	21	15	5	16	29	7
Promoter size analysed (kbp)			1.791	1.222	2.011	2.011	0.736	0.493	2.001	2.001	1.715

3. Discussion

The purpose of this study was investigating the influence of transposons on the expression of genes located in their vicinity. We precisely annotated the transposable elements to identify all siRNAs sharing a sequence identity with them. Further analysis was performed on scaffold 1222 containing a cluster of genes involved in rubber biosynthesis.

3.1. Consequences of TE Location and siRNA Production Nearby in Genes Involved in Natural Rubber Biosynthesis

The scaffold 1222 sequence in clone PB 260 was constructed from clone Reyan 7-33-97 de novo genome. In clone RRIM 600, local variations in gene location were observed in the corresponding scaffold (scaffold 1741 [18] corresponding to contig MKXE01001735.1 in the repository). Conversely, the GT 1 genome showed deep restructuring of the *REF/SRPP* locus.

The systematic presence of TEs in the promoter sequences observed on scaffold 1222 questioned the regulation of *REF* and *SRPP* gene expression. The presence of TEs in the promoter region may confer regulatory *cis*-elements, functionalizing the TEs as part of the promoters, which could also explain variable expression in a tissue-dependent manner. In addition, TEs may also bring alternative transcription start sites (TSS), as shown for clone RRIM 600, where 1/3 of alternative TSS, identified by 5'-CAP sequencing (CAGE), were located no more than two kbp upstream of the transcript at genome level [18]. Alternative TSS may therefore allow the generation of variable protein isoforms for the N-terminal region and long non-coding RNAs [50]. An epigenetic mechanism is at play to repress alternative TSS, based on the methylation of chromatin changes, which is required to maintain precise gene expression control, as demonstrated in eukaryotic genomes [51]. Chromatin marks have the potential to redefine the promoter as an intragenic region, allowing alternative TSS to generate variable protein isoforms for the N-terminal region and/or long non-coding RNAs [50]. In rubber clone PB 260, the next step will be to functionally validate the link between chromatin marks, the presence of TEs, and siRNA production in the environment of genes to demonstrate the transcriptional control of gene expression. Given the large number of TEs in the genome, environmental, developmental and clonal discrepancies in alternative TSS are expected when looking for transcript overlapping promoters and annotating long non-coding RNAs.

TEs are maintained in silent form either by changes in the chromatin structure or directly by cytosine methylation of their sequences in CG, CHG and CHH contexts [52]. DNA methylation in a CHH context is the signature of RNA-directed DNA methylation, RdDM [53,54]. Variation in patterns of methylation within genes and surrounding sequences are associated with a continuous range of expression differences, from silencing to constitutive expression [55]. Methylation around TSS is associated with the silencing of expression [55]. In tomato, a peak of 24-nt siRNA -500 kb upstream of the TSS distribution induced high mCHH [56]. In the rubber, we showed a negative link between siRNA production in the gene body and transcriptional activity of the corresponding gene. It can suggest that the large variation in the level of expression between *REF1*, highly expressed in latex, and *SRPP9*, *SRPP9b* and *SRPP3*, poorly expressed in latex and associated with siRNA production in promoter regions, may be related to a level of CHH methylation. Methylation levels will be assessed on the genomic DNA of bark, comprising latex cells. The collection of latex, corresponding to the cytosol of this specialized cell, only provides easy access to ribonucleic acids (RNAs and small RNAs), as the nuclei remain attached inside.

3.2. TE Diversity in Hevea Clones

All available genomic sequences are from the unrelated Wickam genetic group, with the exception of BPM 24, which is from a GT 1 cross and Reyan 7-33-97 from a RRIM 600 one (<http://rubberclones.cirad.fr/>). In the de novo genomes of rubber clones Reyan 7-33-97 [4], RRIM 600 [18], BPM 24 [6] and GT 1 [5], the repeated regions represent 66%, 69%, 71% and 70% of the genome, respectively, of which 64% to 67% comprise LTR retrotransposons. In contrast, the ratio between the two superfamilies *gypsy*

and *Copia* greatly differed between clones with 6.05 for Reyan 7-33-97, 3.71 for RRIM 600, 3.69 for clone BPM 24 and 3.12 for GT 1. In the present study, the content of repeated elements was higher (75%) in clone PB 260, of which LTR retrotransposons represented 43% of annotated transposons. The *gypsy/Copia* ratio was slightly lower (2.24) in clone PB 260 than other rubber clones. The diversity of TE content and *gypsy/Copia* ratio between rubber clones may be due to the methods used to identify and classify repeated sequences. Indeed, RepeatMasker and RepeatModeler were used for the annotation of the genome from Reyan 7-33-97, BPM 24 and RRIM 600, while the REPET pipeline, combined with LTR_STRUCT, was used for clone PB 260. REPET pipeline was chosen for its sensitivity, by connecting TE fragment even from afar, and its specificity in the detection of TE [46].

The latest reference genome, clone GT 1, was annotated with LTR_FINDER combined with RepeatMasker [5]. As for clone GT 1, the genome size of clone PB 260 increased with the massive expansion of the *Ty3/gypsy Del/Tekay* retroelements.

The size of the genome could also influence the TE content. The genome of Reyan 7-33-97 had an estimated size of about 1.46 Gb, while the size expected for the other clones, measured by flow cytometry, was about 2.15 Gb. For clone PB 260, only re-sequencing data are available and scaffolding was done by mapping reads on the Reyan 7-33-97 reference genome. Analysis bias was therefore possible for PB 260. The genome size and TE content variations between clones may also indicate a dynamic genome with recent events, such as proliferation and/or deletion of repeated sequences. However, these variations cannot be attributed to recent insertional activities of identified LTR retrotransposons, as demonstrated by insertion times in PB 260 and GT 1 [5]. The amplification of *Del/Tekay*, the most redundant LTR retrotransposon lineage that contributed to the increase in the genome size of rubber clone PB 260, occurred between 2 to 10 My, with peaks between 6 to 8 My. This observation may suggest that other forces, such as unequal recombination, deletion, or duplication may be involved in *Hevea* genome reshaping. This point deserves to be further studied, since several agro-physiological traits, such as the natural rubber production potential, reactivity to stimulation by ethephon, the characteristics of the polyisoprene chain lengths, and the ability to adapt to abiotic and biotic stress are clone dependent.

3.3. Post-Transcriptional Activity of TE-Derived siRNAs

We had previously identified 445 transcripts degraded by miRNAs [20]. In this study, we did not identify any targets that were post-transcriptionally regulated by TE-derived siRNAs, consistent with the literature, revealing only translation inhibition and miRNA mimicry. To date, only two kinds of siRNA activities had already been studied. The first one is in *Arabidopsis*, where *Athila* LTR-derived small RNA (siRNA854, 22 nt) was shown to bind the 3'UTR of gene *UBP1b* with subsequent translational inhibition [57]. The same mechanism was shown in a *Drosophila* embryo, where TE-derived small RNAs (piwi RNAs) bind to 3'UTR of *nos* mRNA, with subsequent translational inhibition, giving a protein gradient across the embryo for the proper segment fate [57]. In the case of miRNA mimicry, a long non-coding RNA is expressed by a retrotransposon in rice root, which acts as a decoy mRNA and which traps miRNA171. The removal of post-transcriptional regulation by miRNA171 in roots allows the synthesis of the master regulators of root development, SCARECROW-LIKE transcription factors [58]. In rubber trees, these two types of regulation, translational repression and miRNA mimicry, deserve to be validated by monitoring protein formation. This cannot be done on a large scale, but could be carried out on only a few targets of interest to demonstrate the link between the production dynamics of siRNAs produced by transposons, the identification of their corresponding targets for which proteins will no longer be formed, and the impact of the activation or suppression of post-transcription regulation on cell function in a given physiological context or developmental stage.

4. Materials and Methods

4.1. Clone PB 260 Nuclear Genome Re-Sequencing and Other Genomes Available Used in this Study

Nuclear DNA from leaves of rubber clone PB 260 was sequenced by GATC (<https://www.eurofinngenomics.eu/>) using Illumina pair-end sequencing (2 × 150 bp) [21]. Briefly, a total of 84 Gb was obtained, from which 62 Gb were assembled through alignment against the clone Reyan 7-33-97 reference genome [4]. Unmapped sequences (~200 kbp) were further assembled using the MaSuRCA (Version 3.2.4) mega-reads algorithm [59], by using clone BPM 24 SMRT raw reads [6]. The PB 260 re-sequenced genome assembly used in this study was therefore a combination of two origins of mapped sequences. The re-sequencing data are available under project number PRJCA001333 in the GSA [36] and BIG Data Center [60]. The Overview of genome assembly available and used in this study is in Table 4.

Table 4. Overview of genome assembly available and used in this study.

	Clones	PB 260 ¹	Reyan-7-33-97 ¹	RRIM 600 ¹	GT 1 ¹	BPM 24 ¹
Available data	Genome Assembly	PRJCA001333	LVXX01000000	AJZ000000000	PRJNA587314	BDHL000000000
	WGS data	PRJCA001333	no	AJZ000000000	PRJNA587314	Link1
	SMRT reads	no	no	no	no	Link2
	RNA-seq	PRJCA001333	SRP069104	no	PRJNA587314	no
Experiments described in this study	smRNA-seq	PRJCA001333	no	no	no	no
	TE annotation	this study	[4]	[18]	[5]	[19]
	siRNA quantification	this study	no	no	no	no
	Reconstruction of the SRPP/REF locus	this study	[4]	[18]	[5]	[19]

¹ PB 260 data was deposited to NGDC and other data was deposited to NCBI. Link1 refer to <http://www4a.biotec.or.th/rubber/GenomeSeq>. Link2 refer to <http://www4a.biotec.or.th/rubber/GenomeSeq>.

4.2. Detection of TEs by TEdenovo and LTR_STRUC

From the re-sequenced PB 260 genome assembly, N stretches over 11 nt in length were removed by the dbChunk.py program installed in the REPET pipeline (Version 2.1) [46]. Genomic sequences from clone PB 260 were chunked into 84,218 contigs. Then, 300 Mb, representing the largest 4000 contigs, were used as inputs to the TEdenovo pipeline [61], as recommended to avoid the use of too many informatic resources for very repetitive sequences (V. Jamilloux, personal communication, [62]). TEdenovo consensus nucleotide sequences were classified according to the Repbase database [63] and named by the classification proposed by Wicker's hierarchical TE classification system [64]. The PASTEC program [64] removed chimeric sequences (chim) and no category (nocat). An additional filter was added to delete sequences with a confidence interval (CI) <20. CdHit [65] was used to cluster sequences. Rpt_map in REPET was used to build alignments with a minimum of three sequences in one cluster and dbConsensus.py to obtain consensus in each cluster. Then, all the genomic sequences (1.2 Gb) were used to launch LTR_STRUC [66] with default parameters, in order to detect full-length LTR retrotransposons. Full-length LTR retrotransposon annotation and analyses were performed by INPACTOR [67]. Sequences without clustering were defined as singleton sequences. Combined consensus sequences, without redundancy, performed by the PASTEC program [64] from the three analyses (TEdenovo, LTR_STRUC and singleton), were used as an input for TEannot.

4.3. TE Annotation

Three paths of the TEannot pipeline were needed (Figure 2). The first one, run on the same subset of 300 Mb of genomic sequences, allowed the annotation of full-length fragments and copies. Full-length fragments were used for a second path on the same subset of 300 Mb. A manual curation step was added before the third path. Briefly, alignments against the consensus sequences were checked individually to discard chimeric and badly covered consensus, as well as low complexity sequences. To do so, a plot coverage and a dot-plot were generated for each consensus. Moreover, a phylogenetic analysis with the reverse transcriptase (RT) domains before and after manual curation

allowed validation of the presence of one copy for each lineage and family. The third and last path was run on the 1.2 Gb genomic sequences from clone PB 260. Additional filters were added to delete sequences < 80bp with less than 80% homology [25]. PB260_TE.gff3 and PB260_TE_filtered.gff3 files were generated.

4.4. MITE and SINE Prediction

MITE detection was performed with the MUST program [68] and redundancy was removed by BLASTClust [69]. SINE detection was performed by SINE_finder [70]. The PB 260 genomic sequences were annotated with Censor [71]. The corresponding SINE.gff3 and MITE.gff3 were generated.

4.5. Estimation of Insertion Time for LTR Retrotransposons

The insertion time of full-length copies was estimated based on the divergence of the 5'- and 3'-LTR sequences of each copy [72]. The difference in the Ka/Ks ratio between Cassava and *Hevea* is 0.14 (Cassava 0.37 and *Hevea* 0.23) [4] corresponding to a speciation time of around 36 million years ago dated thanks to a fossil-calibrated molecular clock for the *Euphorbiaceae* [6]. The insertion dates (T) were estimated using the formula $T = Ks/2r$, where T is the time of divergence, Ks is the number of synonymous base substitutions per site and r is the substitution rate [72]. The calculated average base substitution rates per year for coding sequences (r) in *Euphorbiaceae* could therefore be calculated as $Ks/2T = [0.14/(2*36MY)] = 1.94 \times 10^{-9}$. The rate used for the LTR divergence analysis was 2-fold higher (3.89×10^{-9}) than that determined for coding sequences in *Hevea* based on the assumption that non-coding sequences evolve more rapidly [73–76]. Almost intact Target Site Duplication (TSD) at both ends of the elements were kept for the estimation of insertion time. Among them 79.4% show intact TSD, 19% contained one mismatch and 1.5% contained two mismatches.

4.6. TE-Derived siRNA Annotation and Abundance

Five small RNA-seq datasets are available for clone PB 260, from juvenile plants in the greenhouse (leaf, stem, root) to mature plants in the field (from young and mature leaves, from latex of healthy and TPD-affected trees) [35,37,77,78]. Cutadapt was used to remove adapter and low-quality reads. MITP (<https://sourceforge.net/projects/mitp/>) was used to identify the miRNAs [20,21]. The clean siRNA sequences were obtained by removing all predicted miRNAs in clean reads. Blat [79] was used to get the small RNA loci in the PB 260 genome with the parameter “minScore = 10, tileSize = 8”, and “blat_top_hit_extractor.pl” in Trinity [80] was used to ensure the best hit of the blat result. The BEDTOOLS program (2.24.0) was used to intersect the siRNA loci with that of the transposable elements. The PB260_TE_derivedsiRNAs.gff3 file was generated.

4.7. Gene Annotation of the Clone PB 260 Genome

EGN-EP transfer (egn_annotation_transfer.pl) [49] was used to transfer annotations from the reference genome from clone Reyan 7-33-97 to clone PB 260. The PB260_Gene.gff3 file was generated. Full EGN-EP was used to predict genes, combining the mapping of expression data (PB 260 transcriptomes db and NCBI *Euphorbiaceae* EST db) and polypeptide data (Swiss-prot db, Reyan 7-33-97_protein.faa [4] and TrEMBL db). The PB260_Gene_EGNEP.gff3 file was generated. All annotation results were then evaluated by a BUSCO analysis [81].

Post-processing steps were necessary, on the one hand to filter out short (less than 600 bp) and doubtful genes, having either no BLAST hit with the protein databanks (/status = obsolete) or a BLAST hit in Repbase (/transposable_element_gene = 1), and on the other hand to tag the full EGN-EP genes with the EGN-EP transfer results (/homolog = reyan_gene_id) using the Bedtools (Version 2.26.0) intersect [82,83].

4.8. Manual Curation of the Scaffold 1222 Sequence from Clone PB 260

Completeness for scaffold 1222 was checked with clone BPM 24 SMRT reads [19]. Another gene annotation of scaffold 1222 from clone Reyan 7-33-97 was transferred to clone PB 260 by the genome comparison result with RGAAT [84] with default parameters. The analysis of scaffold 1222 was completed by a dot-plot of the Reyan 7-33-97 scaffold against the one for clone PB 260 using Gepard [85]. The schematic representation of the clone PB 260 scaffold 1222 was drawn using DNAPlotter [86].

4.9. RNA-Seq Data Analysis

The RSEM program (Version 1.2.29) was used to calculate the normalized expression of full-length transcripts encoding Rubber Elongation Factor (*REF*) and Small Rubber Particle Protein (*SRPP*) found in scaffold 1222 in clone PB 260. As input, we used latex RNA-seq data [39] generated from three healthy trees without ethephon stimulation (water-treated healthy trees, WH), three healthy and three TPD-affected trees subjected to stress induced by ethephon treatment (ethephon-treated healthy trees, EH, and ethephon-treated TPD-affected trees, ET, respectively).

4.10. Promoter Analysis

A region of 2 kb was extracted, when possible, from the start codon for *REF1*, *REF2*, *REF3*, *REF4*, *REF5*, *REF7*, *REF8*, *SRPP1* and *SRPP5*. The PlantCARE webservice (<http://bioinformatics.psb.ugent.be/webtools/plantcare/html/>) was used to detect *cis*-acting regulatory elements [87].

4.11. Phylogenetic Analysis

Full-length protein sequences of the *SRPP/REF* family were extracted from clones PB 260, Reyan 7-33-97 [4] and *Manihot esculenta* (<https://phytozome.jgi.doe.gov/pz/portal.html>). The MUSCLE program (Version 3.8.31) was used for multiple sequence alignment. The gaps in the alignment were removed using the trimAl program with “-nogaps” (Version 1.4). MrBayes (V3.2.6 x64) was used to build the phylogenetic tree.

4.12. Comparative Genome Analysis

Genomic fragments were compared using Gepard [85]. PB 260 scaffold1222 was compared to the clones Reyan 7-33-97 (scaffold lvxx01001222), RRIM600 (scaffold mkxe01001735) and GT1 (chromosome 9 position 13,437,700-13,754,119 bp).

5. Conclusions

Altogether, these analyses indicated first of all the importance of accurate TE annotation as a priority in plant genome sequencing projects to minimize the inaccuracy of gene annotation and facilitate functional gene studies. This study confirmed that TEs are the main contributors to genome shaping and, as a consequence, to the regulation of genome expression. These analyses are a valuable resource for comparative epi/genomics within the *Euphorbiaceae*, and transposon tagging for designing clone-specific molecular markers in *Hevea*. We had already demonstrated that the natural rubber biosynthesis pathway is under post-transcriptional control [20]. This work shows that this biosynthesis pathway is also under transcriptional control with a major role of TEs, which are functionalized in the promoters of the genes involved in natural rubber biosynthesis.

Supplementary Materials: Supplementary materials can be found at <http://www.mdpi.com/1422-0067/21/12/4220/s1>. Supplementary data 1: Transposable elements expression in RNA-seq data from latex of healthy trees stimulated or not by ethephon; and from latex of TPD-affected trees. Count tables and Deseq 2 analyses are provided. Supplementary data 2: Mapping results of siRNA on annotated transposable elements. Supplementary data 3: Completeness of PB 260 re-sequenced genome annotation, according to the pipeline used, assessed by BUSCO with eudicotyledons_odb10 database. Supplementary data 4: Statistics for PB 260 re-sequenced genome annotation by using the full EGN-EP pipeline. Supplementary Figure S1: Complete phylogenetic analysis, based on amino acid sequences from the reverse transcriptase (RT) domain, when present, on 1476 full-length copies

obtained after LTR_STRUC and Inpactor classification. Supplementary Figure S2: the complete phylogenetic analysis carried out before (A) and after manual curation (B). Supplementary Figure S3. siRNA production by transposable element orders and superfamilies (%). (A) 21-nt siRNA. (B) 22-nt siRNA. (C) 23-nt siRNAs.

Author Contributions: Conceptualization, J.L. and S.W.; methodology, S.W., J.L., R.G. and S.B.; formal analysis, S.W., J.L., G.D. and R.G.; data curation, R.G., S.B. and J.L.; Plant material: P.M. and F.O.; Data from clone Reyan 7-33-97: C.T.; writing—original draft preparation, J.L.; writing—review and editing, S.W., J.L., R.G., S.B.; visualization, S.W., J.L. and R.G.; supervision, J.L., S.H. and P.M.; funding acquisition, P.M., S.H., J.L. and S.W. All authors have read and agreed to the published version of the manuscript.

Funding: S.W. benefited from a scholarship from the UCAS Joint PhD Training Programme. J.L. and S.W. benefited from a mobility program in 2018 from Campus France (Xu Guangqi Programme No. 41241QJ).

Acknowledgments: The authors would like to thank Zheng Li, the CIRAD-INRA representative in Beijing, for his support, and Peter Biggins, a professional translator for careful reading of the manuscript. This work was supported by the CIRAD-UMR AGAP HPC Data Centre of the South Green Bioinformatics platform (<http://www.southgreen.fr/>).

Conflicts of Interest: The authors declare no conflict of interest and the funders had no role in the design of the study; in the collection, analyses, or interpretation of data; in the writing of the manuscript, or in the decision to publish the results.

References

1. Yamashita, S.; Takahashi, S. Molecular Mechanisms of Natural Rubber Biosynthesis. *Annu. Rev. Biochem.* **2020**. [[CrossRef](#)] [[PubMed](#)]
2. Compagnon, P.; Chapuset, T.; Gener, P.; Jacob, J.-L.; De La Serve, M.; De Livonnière, H.; Nicolas, D.; Omont, H.; Serier, J.-B.; Tran Van Canh, C.; et al. *Le Caoutchouc Naturel Biologie, Culture, Production*; Maisonneuve et Larose: Paris, France, 1986; p. 595.
3. Men, X.; Wang, F.; Chen, G.Q.; Zhang, H.B.; Xian, M. Biosynthesis of Natural Rubber: Current State and Perspectives. *Int. J. Mol. Sci.* **2018**, *20*, 50. [[CrossRef](#)] [[PubMed](#)]
4. Tang, C.; Yang, M.; Fang, Y.; Luo, Y.; Gao, S.; Xiao, X.; An, Z.; Zhou, B.; Zhang, B.; Tan, X.; et al. The rubber tree genome reveals new insights into rubber production and species adaptation. *Nat. Plants* **2016**, *2*, 16073. [[CrossRef](#)] [[PubMed](#)]
5. Liu, J.; Shi, C.; Shi, C.C.; Li, W.; Zhang, Q.J.; Zhang, Y.; Li, K.; Lu, H.F.; Shi, C.; Zhu, S.T.; et al. The Chromosome-Based Rubber Tree Genome Provides New Insights into Spurge Genome Evolution and Rubber Biosynthesis. *Mol. Plant* **2020**, *13*, 336–350. [[CrossRef](#)]
6. Deng, Z.; Chen, J.; Leclercq, J.; Zhou, Z.; Liu, C.; Liu, H.; Yang, H.; Montoro, P.; Xia, Z.; Li, D. Expression Profiles, Characterization and Function of HbTCTP in Rubber Tree (*Hevea brasiliensis*). *Front. Plant Sci.* **2016**, *7*, 789. [[CrossRef](#)]
7. Priya, P.; Venkatachalam, P.; Thulaseedharan, A. Differential expression pattern of rubber elongation factor (REF) mRNA transcripts from high and low yielding clones of rubber tree (*Hevea brasiliensis* Muell. Arg.). *Plant Cell Rep.* **2007**, *26*, 1833–1838. [[CrossRef](#)] [[PubMed](#)]
8. Jacob, J.L.; d’Auzac, J.; Prevot, J.C.; Serier, J.B. Une usine à caoutchouc naturel: L’hévéa. *La Rech.* **1995**, *26*, 538–545.
9. Jacob, J.L.; Serres, E.; Prévôt, J.C.; Lacrotte, R.; Vidal, A.; Eschbach, J.M.; D’auzac, J. Development of *Hevea* Latex Diagnosis. *Agritrop* **1988**, *12*, 97–115.
10. Eschbach, J.-M.; Roussel, D.; Van de Sype, H.; Jacob, J.-L.; D’auzac, J. Relationships between yield and clonal physiological characteristics of latex from *Hevea brasiliensis*. *Physiol. Végétale* **1984**, *22*, 294–304.
11. Sreelatha, S.; Mydin, K.; Simon, S.; Jacob, J.; Krishnakumar, R. Biochemical characterisation of RR II 400 series clones of *Hevea brasiliensis*. *Nat. Rubber Res.* **2009**, *22*, 36–42.
12. Prevot, J.; Jacob, J.; Vidal, A. The redox potential of latex: Criterion of the physiological state of the laticiferous system. In Proceedings of the Exploitation, Physiology and Improvement of *Hevea*, Montpellier, France, 9–12 July 1984; pp. 227–238.
13. Zhang, Y.; Leclercq, J.; Montoro, P. Reactive oxygen species in *Hevea brasiliensis* latex and relevance to Tapping Panel Dryness. *Tree Physiol.* **2017**, *37*, 261–269. [[CrossRef](#)] [[PubMed](#)]
14. Lacote, R.; Gabla, O.; Obouayeba, S.; Eschbach, J.M.; Rivano, F.; Dian, K.; Gohet, E. Long-term effect of ethylene stimulation on the yield of rubber trees is linked to latex cell biochemistry. *Field Crop. Res.* **2010**, *115*, 94–98. [[CrossRef](#)]

15. Chrestin, H. Biochemical aspects of bark dryness induced by overstimulation of rubber trees with Ethrel. In *Physiology of Rubber Tree Latex*; d'Auzac, J., Jacob, J.L., Chrestin, H., Eds.; CRC Press: Boca Raton, FL, USA, 1989; pp. 432–439.
16. Yang, S.Q.; Fan, X.W. Physiological response of PR107 to intensive tapping with stimulation at early exploitation stage. *Chin. J. Trop. Crop. Res.* **1995**, *16*, 17–28.
17. Piyatrakul, P.; Putranto, R.A.; Martin, F.; Rio, M.; Dessailly, F.; Leclercq, J.; Dufayard, J.F.; Lardet, L.; Montoro, P. Some ethylene biosynthesis and AP2/ERF genes reveal a specific pattern of expression during somatic embryogenesis in *Hevea brasiliensis*. *BMC Plant Biol.* **2012**, *12*, 244. [[CrossRef](#)]
18. Lau, N.S.; Makita, Y.; Kawashima, M.; Taylor, T.D.; Kondo, S.; Othman, A.S.; Shu-Chien, A.C.; Matsui, M. The rubber tree genome shows expansion of gene family associated with rubber biosynthesis. *Sci. Rep.* **2016**, *6*, 28594. [[CrossRef](#)]
19. Pootakham, W.; Sonthirod, C.; Naktang, C.; Ruang-Areerate, P.; Yoocha, T.; Sangsrakru, D.; Theerawattanasuk, K.; Rattanawong, R.; Lekawipat, N.; Tangphatsornruang, S. De novo hybrid assembly of the rubber tree genome reveals evidence of paleotetraploidy in *Hevea* species. *Sci. Rep.* **2017**, *7*, 41457. [[CrossRef](#)]
20. Leclercq, J.; Wu, S.; Farinas, B.; Pointet, S.; Favreau, B.; Vignes, H.; Kuswanhadi, K.; Ortega-Abboud, E.; Dufayard, J.F.; Gao, S.; et al. Post-transcriptional regulation of several biological processes involved in latex production in *Hevea brasiliensis*. *PeerJ* **2020**, *8*. [[CrossRef](#)]
21. Zhang, Y.; Leclercq, J.; Wu, S.; Ortega-Abboud, E.; Pointet, S.; Tang, C.; Hu, S.; Montoro, P. Genome-wide analysis in *Hevea brasiliensis* laticifers revealed species-specific post-transcriptional regulations of several redox-related genes. *Sci. Rep.* **2019**, *9*, 5701. [[CrossRef](#)]
22. Wei, L.; Cao, X. The effect of transposable elements on phenotypic variation: Insights from plants to humans. *Sci. China Life Sci.* **2016**, *59*, 24–37. [[CrossRef](#)]
23. Galindo-Gonzalez, L.; Mhiri, C.; Deyholos, M.K.; Grandbastien, M.A. LTR-retrotransposons in plants: Engines of evolution. *Gene* **2017**, *626*, 14–25. [[CrossRef](#)]
24. Vicient, C.M.; Casacuberta, J.M. Impact of transposable elements on polyploid plant genomes. *Ann. Bot.* **2017**, *120*, 195–207. [[CrossRef](#)] [[PubMed](#)]
25. Wicker, T.; Sabot, F.; Hua-Van, A.; Bennetzen, J.L.; Capy, P.; Chalhoub, B.; Flavell, A.; Leroy, P.; Morgante, M.; Panaud, O.; et al. A unified classification system for eukaryotic transposable elements. *Nat. Rev. Genet.* **2007**, *8*, 973–982. [[CrossRef](#)] [[PubMed](#)]
26. Du, J.; Tian, Z.; Hans, C.S.; Laten, H.M.; Cannon, S.B.; Jackson, S.A.; Shoemaker, R.C.; Ma, J. Evolutionary conservation, diversity and specificity of LTR-retrotransposons in flowering plants: Insights from genome-wide analysis and multi-specific comparison. *Plant J.* **2010**, *63*, 584–598. [[CrossRef](#)]
27. Llorens, C.; Futami, R.; Covelli, L.; Dominguez-Escriba, L.; Viu, J.M.; Tamarit, D.; Aguilar-Rodriguez, J.; Vicente-Ripolles, M.; Fuster, G.; Bernet, G.P.; et al. The Gypsy Database (GyDB) of mobile genetic elements: Release 2.0. *Nucleic Acids Res.* **2011**, *39*, D70–D74. [[CrossRef](#)] [[PubMed](#)]
28. Domingues, D.S.; Cruz, G.M.; Metcalfe, C.J.; Nogueira, F.T.; Vicentini, R.; Alves Cde, S.; Van Sluys, M.A. Analysis of plant LTR-retrotransposons at the fine-scale family level reveals individual molecular patterns. *BMC Genom.* **2012**, *13*, 137. [[CrossRef](#)]
29. Xu, Z.; Liu, J.; Ni, W.; Peng, Z.; Guo, Y.; Ye, W.; Huang, F.; Zhang, X.; Xu, P.; Guo, Q.; et al. GrTEdb: The first web-based database of transposable elements in cotton (*Gossypium raimondii*). *Database J. Biol. Databases Curation* **2017**, 2017. [[CrossRef](#)] [[PubMed](#)]
30. Beule, T.; Agbessi, M.D.; Dussert, S.; Jaligot, E.; Guyot, R. Genome-wide analysis of LTR-retrotransposons in oil palm. *BMC Genom.* **2015**, *16*, 795. [[CrossRef](#)]
31. Ming, R.; Wai, C.M.; Guyot, R. Pineapple Genome: A Reference for Monocots and CAM Photosynthesis. *Trends Genet. TIG* **2016**, *32*, 690–696. [[CrossRef](#)]
32. Kumar, A.; Bennetzen, J.L. Plant retrotransposons. *Annu. Rev. Genet.* **1999**, *33*, 479–532. [[CrossRef](#)]
33. Neumann, P.; Novak, P.; Hostakova, N.; Macas, J. Systematic survey of plant LTR-retrotransposons elucidates phylogenetic relationships of their polyprotein domains and provides a reference for element classification. *Mob. DNA-UK* **2019**, *10*. [[CrossRef](#)]
34. Bologna, N.G.; Voinnet, O. The diversity, biogenesis, and activities of endogenous silencing small RNAs in Arabidopsis. *Annu. Rev. Plant Biol.* **2014**, *65*, 473–503. [[CrossRef](#)] [[PubMed](#)]

35. Gébelin, V.; Argout, X.; Engchuan, W.; Pitollat, B.; Duan, C.; Montoro, P.; Leclercq, J. Identification of novel microRNAs in *Hevea brasiliensis* and computational prediction of their targets. *BMC Plant Biol.* **2012**, *12*, 18. [[CrossRef](#)] [[PubMed](#)]
36. Gébelin, V.; Leclercq, J.; Hu, S.; Tang, C.; Montoro, P. Regulation of *MIR* genes in response to abiotic stress in *Hevea brasiliensis*. *Int. J. Mol. Sci.* **2013**, *14*, 19587–19604. [[CrossRef](#)] [[PubMed](#)]
37. Gébelin, V.; Leclercq, J.; Kuswanhadi; Argout, X.; Chaidamsari, T.; Hu, S.; Tang, C.; Sarah, G.; Yang, M.; Montoro, P. The small RNA profile in latex from *Hevea brasiliensis* trees is affected by tapping panel dryness. *Tree Physiol.* **2013**, *33*, 1084–1098. [[CrossRef](#)]
38. Duan, C.; Argout, X.; Gebelin, V.; Summo, M.; Dufayard, J.F.; Leclercq, J.; Hadi, K.; Piyatrakul, P.; Pirrello, J.; Rio, M.; et al. Identification of the *Hevea brasiliensis* AP2/ERF superfamily by RNA sequencing. *BMC Genom.* **2013**, *14*, 30. [[CrossRef](#)]
39. Montoro, P.; Wu, S.; Favreau, B.; Herlinawati, E.; Labrune, C.; Martin-Magniette, M.L.; Pointet, S.; Rio, M.; Leclercq, J.; Ismawanto, S.; et al. Transcriptome analysis in *Hevea brasiliensis* latex revealed changes in hormone signalling pathways during ethephon stimulation and consequent Tapping Panel Dryness. *Sci. Rep.* **2018**, *8*, 8483. [[CrossRef](#)]
40. Leclercq, J.; Lardet, L.; Martin, F.; Chapuset, T.; Oliver, G.; Montoro, P. The green fluorescent protein as an efficient selection marker for *Agrobacterium tumefaciens*-mediated transformation in *Hevea brasiliensis* (*Mull. Arg.*). *Plant Cell Rep.* **2010**, *29*, 513–522. [[CrossRef](#)]
41. Leclercq, J.; Martin, F.; Sanier, C.; Clement-Vidal, A.; Fabre, D.; Oliver, G.; Lardet, L.; Ayar, A.; Peyramard, M.; Montoro, P. Over-expression of a cytosolic isoform of the *HbCuZnSOD* gene in *Hevea brasiliensis* changes its response to a water deficit. *Plant Mol. Biol.* **2012**, *80*, 255–272. [[CrossRef](#)]
42. Lestari, R.; Rio, M.; Martin, F.; Leclercq, J.; Woraathasin, N.; Roques, S.; Dessailly, F.; Clement-Vidal, A.; Sanier, C.; Fabre, D.; et al. Overexpression of *Hevea brasiliensis* ethylene response factor *HbERF-IXc5* enhances growth and tolerance to abiotic stress and affects laticifer differentiation. *Plant Biotechnol. J.* **2018**, *16*, 322–336. [[CrossRef](#)]
43. Martin, F.; Abati, V.; Burel, A.; Clement-Vidal, A.; Sanier, C.; Fabre, D.; Woraathasin, N.; Rio, M.; Besret, P.; Farinas, B.; et al. Overexpression of *EcGSH1* induces glutathione production and alters somatic embryogenesis and plant development in *Hevea brasiliensis*. *Ind. Crop. Prod.* **2018**, *112*, 803–814. [[CrossRef](#)]
44. Montoro, P.; Rattana, W.; Pujade-Renaud, V.; Michaux-Ferriere, N.; Monkolsook, Y.; Kanthapura, R.; Adunsadthapong, S. Production of *Hevea brasiliensis* transgenic embryogenic callus lines by *Agrobacterium tumefaciens*: Roles of calcium. *Plant Cell Rep.* **2003**, *21*, 1095–1102. [[CrossRef](#)] [[PubMed](#)]
45. Montoro, P.; Teinseree, N.; Rattana, W.; Kongsawadworakul, P.; Michaux-Ferriere, N. Effect of exogenous calcium on *Agrobacterium tumefaciens*-mediated gene transfer in *Hevea brasiliensis* (rubber tree) friable calli. *Plant Cell Rep.* **2000**, *19*, 851–855. [[CrossRef](#)]
46. Flûtre, T.; Duprat, E.; Feuillet, C.; Quesneville, H. Considering transposable element diversification in de novo annotation approaches. *PLoS ONE* **2011**, *6*, e16526. [[CrossRef](#)] [[PubMed](#)]
47. Uthup, T.K.; Saha, T.; Ravindran, M.; Bini, K. Impact of an intragenic retrotransposon on the structural integrity and evolution of a major isoprenoid biosynthesis pathway gene in *Hevea brasiliensis*. *Plant Physiol. Biochem.* **2013**, *73*, 176–188. [[CrossRef](#)]
48. Schulman, A.H. Retrotransposon replication in plants. *Curr. Opin. Virol.* **2013**, *3*, 604–614. [[CrossRef](#)] [[PubMed](#)]
49. Sallet, E.; Gouzy, J.; Schiex, T. EuGene: An Automated Integrative Gene Finder for Eukaryotes and Prokaryotes. *Methods Mol. Biol.* **2019**, *1962*, 97–120. [[CrossRef](#)] [[PubMed](#)]
50. Nielsen, M.; Ard, R.; Leng, X.; Ivanov, M.; Kindgren, P.; Pelechano, V.; Marquardt, S. Transcription-driven chromatin repression of Intragenic transcription start sites. *PLoS Genet.* **2019**, *15*, e1007969. [[CrossRef](#)]
51. Soares, L.M.; He, P.C.; Chun, Y.; Suh, H.; Kim, T.; Buratowski, S. Determinants of Histone H3K4 Methylation Patterns. *Mol. Cell* **2017**, *68*, 773–785.e6. [[CrossRef](#)]
52. Montgomery, S.A.; Tanizawa, Y.; Galik, B.; Wang, N.; Ito, T.; Mochizuki, T.; Akimcheva, S.; Bowman, J.L.; Cognat, V.; Marechal-Drouard, L.; et al. Chromatin Organization in Early Land Plants Reveals an Ancestral Association between H3K27me3, Transposons, and Constitutive Heterochromatin. *Curr. Biol.* **2020**. [[CrossRef](#)]
53. Bouyer, D.; Kramdi, A.; Kassam, M.; Heese, M.; Schnittger, A.; Roudier, F.; Colot, V. DNA methylation dynamics during early plant life. *Genome Biol.* **2017**, *18*, 179. [[CrossRef](#)]

54. Niederhuth, C.E.; Schmitz, R.J. Putting DNA methylation in context: From genomes to gene expression in plants. *Biochim. Et Biophys. Acta Gene Regul. Mech.* **2017**, *1860*, 149–156. [[CrossRef](#)] [[PubMed](#)]
55. Bewick, A.J.; Ji, L.; Niederhuth, C.E.; Willing, E.M.; Hofmeister, B.T.; Shi, X.; Wang, L.; Lu, Z.; Rohr, N.A.; Hartwig, B.; et al. On the origin and evolutionary consequences of gene body DNA methylation. *Proc. Natl. Acad. Sci. USA* **2016**, *113*, 9111–9116. [[CrossRef](#)] [[PubMed](#)]
56. Corem, S.; Doron-Faigenboim, A.; Jouffroy, O.; Maumus, F.; Arazi, T.; Bouche, N. Redistribution of CHH Methylation and Small Interfering RNAs across the Genome of Tomato ddm1 Mutants. *Plant Cell* **2018**, *30*, 1628–1644. [[CrossRef](#)] [[PubMed](#)]
57. McCue, A.D.; Slotkin, R.K. Transposable element small RNAs as regulators of gene expression. *Trends Genet. TIG* **2012**, *28*, 616–623. [[CrossRef](#)]
58. Cho, J. Transposon-Derived Non-coding RNAs and Their Function in Plants. *Front. Plant Sci.* **2018**, *9*, 600. [[CrossRef](#)] [[PubMed](#)]
59. Zimin, A.; Puiu, D.; Luo, M.; Zhu, T.; Koren, S.; Marçais, G.; Yorke, J.; Dvořák, J.; Salzberg, S. Hybrid assembly of the large and highly repetitive genome of *Aegilops tauschii*, a progenitor of bread wheat, with the MaSuRCA mega-reads algorithm. *Genome Res.* **2017**, *27*, 787–792. [[CrossRef](#)]
60. Big Data Center Members. Database Resources of the BIG Data Center in 2018. *Nucleic Acids Res.* **2018**, *46*, D14–D20. [[CrossRef](#)] [[PubMed](#)]
61. Permal, E.; Flutre, T.; Quesneville, H. Roadmap for annotating transposable elements in eukaryote genomes. *Methods Mol. Biol.* **2012**, *859*, 53–68. [[CrossRef](#)]
62. Jamilloux, V.; Daron, J.; Choulet, F.; Quesneville, H. De Novo Annotation of Transposable Elements: Tackling the Fat Genome Issue. *Proc. IEEE* **2017**, *105*, 474–481. [[CrossRef](#)]
63. Bao, W.; Kojima, K.; Kohany, O. Repbase Update, a database of repetitive elements in eukaryotic genomes. *Mob. DNA* **2015**, *6*, 11. [[CrossRef](#)]
64. Hoede, C.; Arnoux, S.; Moisset, M.; Chaumier, T.; Inizan, O.; Jamilloux, V.; Quesneville, H. PASTEC: An Automatic Transposable Element Classification Tool. *PLoS ONE* **2014**, *9*, e91929. [[CrossRef](#)] [[PubMed](#)]
65. Fu, L.; Niu, B.; Zhu, Z.; Wu, S.; Li, W. CD-HIT: Accelerated for clustering the next-generation sequencing data. *Bioinformatics* **2012**, *28*, 3150–3152. [[CrossRef](#)] [[PubMed](#)]
66. McCarthy, E.; McDonald, J. LTR_STRUC: A novel search and identification program for LTR retrotransposons. *Bioinformatics* **2003**, *19*, 362–367. [[CrossRef](#)] [[PubMed](#)]
67. Orozco-Arias, S.; Liu, J.; Tabares-Soto, R.; Ceballos, D.; Silva Domingues, D.; Garavito, A.; Ming, R.; Guyot, R. Inpactor, Integrated and Parallel Analyzer and Classifier of LTR Retrotransposons and Its Application for Pineapple LTR Retrotransposons Diversity and Dynamics. *Biology* **2018**, *7*, 32. [[CrossRef](#)] [[PubMed](#)]
68. Ge, R.; Mai, G.; Zhang, R.; Wu, X.; Wu, Q.; Zhou, F. MUSTv2: An Improved De Novo Detection Program for Recently Active Miniature Inverted Repeat Transposable Elements (MITEs). *J. Integr. Bioinform.* **2017**, *14*. [[CrossRef](#)] [[PubMed](#)]
69. Altschul, S.F.; Gish, W.; Miller, W.; Myers, E.W.; Lipman, D.J. Basic local alignment search tool. *J. Mol. Biol.* **1990**, *215*, 403–410. [[CrossRef](#)]
70. Wenke, T.; Dobel, T.; Sorensen, T.R.; Junghans, H.; Weisshaar, B.; Schmidt, T. Targeted Identification of Short Interspersed Nuclear Element Families Shows Their Widespread Existence and Extreme Heterogeneity in Plant Genomes. *Plant Cell* **2011**, *23*, 3117–3128. [[CrossRef](#)]
71. Kohany, O.; Gentles, A.J.; Hankus, L.; Jurka, J. Annotation, submission and screening of repetitive elements in Repbase: RepbaseSubmitter and Censor. *BMC Bioinform.* **2006**, *7*, 474. [[CrossRef](#)]
72. SanMiguel, P.; Gaut, B.S.; Tikhonov, A.; Nakajima, Y.; Bennetzen, J.L. The paleontology of intergene retrotransposons of maize. *Nat. Genet.* **1998**, *20*, 43–45. [[CrossRef](#)]
73. Vitte, C.; Ishii, T.; Lamy, F.; Brar, D.; Panaud, O. Genomic paleontology provides evidence for two distinct origins of Asian rice (*Oryza sativa* L.). *Mol. Genet. Genom. MGG* **2004**, *272*, 504–511. [[CrossRef](#)]
74. Baurens, F.C.; Bocs, S.; Rouard, M.; Matsumoto, T.; Miller, R.N.; Rodier-Goud, M.; Mbéguié-A-Mbéguié, D.; Yahiaoui, N. Mechanisms of haplotype divergence at the RGA08 nucleotide-binding leucine-rich repeat gene locus in wild banana (*Musa balbisiana*). *BMC Plant Biol.* **2010**, *10*, 149. [[CrossRef](#)] [[PubMed](#)]
75. Lescot, M.; Piffanelli, P.; Ciampi, A.Y.; Ruiz, M.; Blanc, G.; Leebens-Mack, J.; da Silva, F.R.; Santos, C.M.; D'Hont, A.; Garsmeur, O.; et al. Insights into the *Musa* genome: Syntenic relationships to rice and between *Musa* species. *BMC Genom.* **2008**, *9*, 58. [[CrossRef](#)] [[PubMed](#)]

76. Ma, J.; Devos, K.M.; Bennetzen, J.L. Analyses of LTR-retrotransposon structures reveal recent and rapid genomic DNA loss in rice. *Genome Res.* **2004**, *14*, 860–869. [[CrossRef](#)] [[PubMed](#)]
77. Kanjanawattanawong, S.; Tangphatsornruang, S.; Triwitayakorn, K.; Ruang-areerate, P.; Sangsrakru, D.; Poopear, S.; Somyong, S.; Narangajavana, J. Characterization of rubber tree microRNA in phytohormone response using large genomic DNA libraries, promoter sequence and gene expression analysis. *Mol. Genet. Genom. MGG* **2014**, *289*, 921–933. [[CrossRef](#)]
78. Lertpanyasampatha, M.; Gao, L.; Kongsawadworakul, P.; Viboonjun, U.; Chrestin, H.; Liu, R.; Chen, X.; Narangajavana, J. Genome-wide analysis of microRNAs in rubber tree (*Hevea brasiliensis* L.) using high-throughput sequencing. *Planta* **2012**, *236*, 437–445. [[CrossRef](#)]
79. Kent, W.J. BLAT—the BLAST-like alignment tool. *Genome Res.* **2002**, *12*, 656–664. [[CrossRef](#)]
80. Grabherr, M.G.; Haas, B.J.; Yassour, M.; Levin, J.Z.; Thompson, D.A.; Amit, I.; Adiconis, X.; Fan, L.; Raychowdhury, R.; Zeng, Q.; et al. Full-length transcriptome assembly from RNA-Seq data without a reference genome. *Nat. Biotechnol.* **2011**, *29*, 644–652. [[CrossRef](#)]
81. Waterhouse, R.M.; Seppey, M.; Simao, F.A.; Manni, M.; Ioannidis, P.; Klioutchnikov, G.; Kriventseva, E.V.; Zdobnov, E.M. BUSCO applications from quality assessments to gene prediction and phylogenomics. *Mol. Biol. Evol.* **2017**. [[CrossRef](#)]
82. Quinlan, A.R. BEDTools: The Swiss-Army Tool for Genome Feature Analysis. *Curr. Protoc. Bioinform.* **2014**, *47*, 11–12. [[CrossRef](#)]
83. Quinlan, A.R.; Hall, I.M. BEDTools: A flexible suite of utilities for comparing genomic features. *Bioinformatics* **2010**, *26*, 841–842. [[CrossRef](#)]
84. Liu, W.; Wu, S.; Lin, Q.; Gao, S.; Ding, F.; Zhang, X.; Aljohi, A.H.; Yu, J.; Hu, S. RGAAT: A Reference-based Genome Assembly and Annotation Tool for New Genomes and Upgrade of Known Genomes. *Genom. Proteom. Bioinform.* **2018**, *16*, 373–381. [[CrossRef](#)] [[PubMed](#)]
85. Krumsiek, J.; Arnold, R.; Rattei, T. Gepard: A rapid and sensitive tool for creating dotplots on genome scale. *Bioinformatics* **2007**, *23*, 1026–1028. [[CrossRef](#)] [[PubMed](#)]
86. Carver, T.; Thomson, N.; Bleasby, A.; Berriman, M.; Parkhill, J. DNAPlotter: Circular and linear interactive genome visualization. *Bioinformatics* **2009**, *25*, 119–120. [[CrossRef](#)] [[PubMed](#)]
87. Lescot, M.; Dehais, P.; Thijs, G.; Marchal, K.; Moreau, Y.; Van de Peer, Y.; Rouze, P.; Rombauts, S. PlantCARE, a database of plant cis-acting regulatory elements and a portal to tools for in silico analysis of promoter sequences. *Nucleic Acids Res.* **2002**, *30*, 325–327. [[CrossRef](#)] [[PubMed](#)]



© 2020 by the authors. Licensee MDPI, Basel, Switzerland. This article is an open access article distributed under the terms and conditions of the Creative Commons Attribution (CC BY) license (<http://creativecommons.org/licenses/by/4.0/>).